Solvation Structures and Kinetics of Solvent Exchange Reactions of the Manganese(II) Ion in Six Nitriles As Studied by X-ray Diffraction, EXAFS, and NMR Techniques

Yasuhiro Inada,[†] Takashi Sugata,[†] Kazuhiko Ozutsumi,[‡] and Shigenobu Funahashi*[,†]

Laboratory of Analytical Chemistry, Faculty of Science, Nagoya University, Chikusa, Nagoya 464-8602, Japan, and Department of Chemistry, Faculty of Science and Engineering, Ritsumeikan University, Kusatsu, Shiga 525-77, Japan

Received July 3, 1997

The solution structure of the manganese(II) ion in acetonitrile (methyl cyanide, AN) has been determined by an X-ray diffraction technique: there are 6.0 ± 0.2 Mn−N bonds and the Mn−N bond length is 221 ± 1 pm. The solvation structures of the manganese(II) ion in propiononitrile (ethyl cyanide, PN), butyronitrile (propyl cyanide, BuN), isobutyronitrile (isopropyl cyanide, ^{i}BuN), valeronitrile (butyl cyanide, VN), and benzonitrile (phenyl cyanide, BzN) have been determined by extended X-ray absorption fine structure spectroscopy. The manganese(II) ion in all of these nitriles is six-coordinate octahedral with an Mn−N bond length of 221 ± 1 pm. The activation parameters for solvent exchange on the manganese(II) ion in the six nitriles have been determined by the nuclear magnetic resonance line broadening technique at various temperatures and pressures. The values of the rate constant (k_{ex}^{298}, s^{-1}), activation enthalpy ($\Delta H^{\ddagger}$, kJ mol^{-1}), activation entropy ($\Delta S^{\ddagger}$, J mol^{-1} K^{-1}), and activation volume ($\Delta V^{\ddagger}$, cm^3 mol^{-1}) for the nitrile exchange are 1.3×10^7, 28.6 ± 0.5, −13 ± 2, and −5.8 ± 0.2 in AN; 1.3×10^7, 29.6 ± 0.7, −10 ± 3, and −2.1 ± 0.4 in PN; 9.9×10^6, 31.3 ± 0.8, −6 ± 3, and −5.0 ± 0.8 in BuN; 1.1×10^7, 40.0 ± 0.4, 24 ± 1, and −2.5 ± 0.7 in ^{i}BuN; 9.3×10^6, 35.6 ± 0.7, 8 ± 3, and +0.6 ± 0.6 in VN; 1.2×10^7, 36.9 ± 0.8, 14 ± 3, and none in BzN, respectively. The values of $\Delta H^{\ddagger}$ and $\Delta S^{\ddagger}$ gradually increase with increasing bulkiness of the nitrile molecule, and the reaction mechanism is concluded to be less associative with increasing the bulkiness, because the Mn−N bond energy in the nitrile-solvated manganese(II) ion is similar in all nitriles. The change in the $\Delta V^{\ddagger}$ value is discussed in terms of the change in the size of the inner sphere.

Introduction

The solvent exchange reaction is one of the most basic chemical reactions of metal ions in solution, and its mechanism has been widely investigated in order to characterize the reactivities of the metal ion.[1] The activation parameters of the solvent exchange reaction such as activation enthalpy ($\Delta H^{\ddagger}$), activation entropy ($\Delta S^{\ddagger}$), and activation volume ($\Delta V^{\ddagger}$) provide valuable information in order to evaluate the reaction mechanisms of the substitution at metal ions. For the first-row transition metal(II) ions, the activation parameters for solvent exchange in water and some nonaqueous solvents have been measured by means of the nuclear magnetic resonance (NMR) line broadening method at various temperatures and pressures. Merbach *et al.* have pointed out that the water exchange reaction proceeds *via* the associative mode for earlier transition metal(II) ions such as vanadium(II) and manganese(II) ions and that the mechanism progressively changes to dissociative for later transition metal(II) ions such as cobalt(II) and nickel(II) ions.[2] Recently, the reaction mechanisms for the water exchange of some metal(II,III) ions have been studied by the *ab initio* molecular orbital calculations,[3] and the correlation between the reaction mechanism and the value of $\Delta V^{\ddagger}$ has been demonstrated.[3a,b,i] According to the results, it is theoretically suggested that the water exchange on the manganese(II) ion proceeds *via* an associative interchange pathway. Because the negative $\Delta V^{\ddagger}$ value has been observed in methanol (−5.0 cm^3 mol^{-1})[4] and acetonitrile (−7.0 cm^3 mol^{-1})[5] for the manganese(II) ion besides in water ($\Delta V^{\ddagger}$ = −6.2 cm^3 mol^{-1}),[2] the solvent exchange mechanisms in these small nonaqueous solvents are also regarded as an associative interchange.

In bulkier solvents, the solvent exchange mechanism of the manganese(II) ion will become less associative and the $\Delta V^{\ddagger}$ value is expected to increase. In fact, the $\Delta V^{\ddagger}$ values were previously determined in bulky solvents, such as *N*,*N*-dimethylformamide (+1.6 cm^3 mol^{-1}),[6] acetic acid (+0.4 cm^3 mol^{-1}),[7] and *N*,*N*-dimethylthioformamide (+11.5 cm^3 mol^{-1}),[8] which

* Corresponding author. E-mail: sfuna@chem4.chem.nagoya-u.ac.jp.
† Nagoya University.
‡ Ritsumeikan University.

(1) (a) Wilkins, R. G. *Kinetics and Mechanisms of Reactions of Transition Metal Complexes*, 2nd ed.; VCH Publishers: New York, 1991. (b) Jordan, R. B. *Reaction Mechanisms of Inorganic and Organometallic Systems*; Oxford University Press: New York, 1991. (c) Burgess, J. *Metal Ions in Solution*; John Wiley & Sons: New York, 1978.
(2) (a) Merbach, A. E. *Pure Appl. Chem.* **1982**, *54*, 1479. (b) Merbach, A. E. *Pure Appl. Chem.* **1987**, *59*, 161. (c) Lincoln, S. F.; Merbach, A. E. *Adv. Inorg. Chem.* **1995**, *42*, 1.
(3) (a) Rotzinger, F. P. *J. Am. Chem. Soc.* **1997**, *119*, 5230. (b) Rotzinger, F. P. *J. Am. Chem. Soc.* **1996**, *118*, 6760. (c) Tsutsui, Y.; Wasada, H.; Funahashi, S. *Bull. Chem. Soc. Jpn.* **1997**, *70*, 1813. (d) Åkesson, R.; Pettersson, L. G. M.; Sandström, M.; Wahlgren, U. *J. Am. Chem. Soc.* **1994**, *116*, 8705. (e) Åkesson, R.; Pettersson, L. G. M.; Sandström, M.; Siegbahn, P. E. M.; Wahlgren, U. *J. Phys. Chem.* **1993**, *97*, 3765. (f) Kang, S.-K.; Lam, B.; Albright, T. A.; O'Brien, J. F. *New J. Chem.* **1991**, *15*, 757. (g) Deeth, R. J.; Elding, L. I. *Inorg. Chem.* **1996**, *35*, 5019. (h) Lee, M. A.; Winter, N. W.; Casev, W. H. *J. Phys. Chem.* **1994**, *98*, 8641. (i) Hartmann, M.; Clark, T.; van Eldik, R. *J. Am. Chem. Soc.* **1997**, *119*, 7843.
(4) Meyer, F. K.; Newman, K. E.; Merbach, A. E. *J. Am. Chem. Soc.* **1979**, *101*, 5588.
(5) Sisley, M. J.; Yano, Y.; Swaddle, T. W. *Inorg. Chem.* **1982**, *21*, 1141.
(6) Ishii, M.; Funahashi, S.; Tanaka, M. *Chem. Lett.* **1987**, 871.
(7) Ishii, M.; Funahashi, S.; Tanaka, M. *Inorg. Chem.* **1988**, *27*, 3192.
(8) Moore, P.; Fielding, L. *J. Chem. Soc., Chem. Commun.* **1988**, 49.

S0020-1669(97)00830-6 CCC: $15.00
Published on Web 04/01/1998

were discussed in terms of the bulkiness of solvent molecules causing the mechanism to be less associative. In this work, to evaluate the change in the reaction mechanisms and the $\Delta V^{\ddagger}$ values with variation in the bulkiness of the solvent molecules, we have studied the solvent exchange reactions of the manganese(II) ion in six nitriles with different sizes of the alkyl or aryl substituent, *i.e.*, acetonitrile (methyl cyanide, AN), propiononitrile (ethyl cyanide, PN), butyronitrile (propyl cyanide, BuN), isobutyronitrile (isopropyl cyanide, ^{i}BuN), valeronitrile (butyl cyanide, VN), and benzonitrile (phenyl cyanide, BzN).

When the solvent exchange rate of the metal ion is measured by the NMR line broadening technique, its solvation structure should be determined, because the coordination number of the metal ion is important when evaluating the solvent exchange rate constants and the reaction mechanisms.[9] In many solvents, the solvation structure of the manganese(II) ion has been determined to be 6-coordinate octahedral using the X-ray diffraction (XD) technique and extended X-ray absorption fine structure (EXAFS) spectroscopy.[10−13] We also know that the bulkiness of the solvent molecule may change the solvation structure; for example, the solvation structures of the first-row transition metal(II) ions in 1,1,3,3-tetramethylurea are not 6-coordinate octahedral.[14] Therefore, first of all, we have determined the solvation structure of the manganese(II) ion in AN by the XD technique and those in the other nitriles by the EXAFS technique. The structure parameters obtained are very important information for the ground state of the nitrile exchange reaction.

Experimental Section

Solvents. AN (Wako), PN (Wako), BuN (Tokyo Chemical), ^{i}BuN (Tokyo Chemical), and VN (Tokyo Chemical) were distilled twice after refluxing for 1 h in the presence of P_2O_5. BzN (Wako) was dried over P_2O_5 for 12 h and distilled twice under reduced pressure. The amount of water in the solvent was confirmed to be less than 3×10^{-3} mol kg^{-1} by the Karl Fisher titration method.

$[Mn(H_2O)_6](CF_3SO_3)_2$. Hydrated manganese(II) trifluoromethanesulfonate was prepared by dropping an aqueous solution of trifluoromethanesulfonic acid into a manganese(II) carbonate suspension in water. The resulting solution was filtered and concentrated. The salt obtained by cooling was recrystallized from water and dried *in vacuo* at room temperature. Found: C, 5.34; H, 2.56. Calcd for $[Mn(H_2O)_6](CF_3SO_3)_2$: C, 5.21; H, 2.62.

Preparation of Sample Solutions. AN and PN solutions of the manganese(II) ion were prepared by dissolving $[Mn(H_2O)_6](CF_3SO_3)_2$ in each solvent, and the water present was then removed by refluxing in a modified Soxhlet extractor with activated 4 Å molecular sieves.[15] In the case of the other nitriles, adequate amounts of $[Mn(H_2O)_6](CF_3SO_3)_2$ were dissolved in BuN, ^{i}BuN, VN, and BzN, and the solutions were allowed to stand over 4 Å molecular sieves under an argon atmosphere for several days. This drying was repeated until the amount of water in solution became negligible relative to the concentration of manganese(II) ion. The manganese(II) ion concentration in each solution was determined by EDTA titration.

Table 1. Structure Parameters around Manganese(II) Ion Determined by X-ray Diffraction and EXAFS Techniques

solvent	concn (mol kg^{-1})	interaction	r (pm)	b or σ^2 (pm^2)	n
AN[a]	0.465[b]	Mn−N	221 ± 1	70 ± 20	6.0 ± 0.2
		Mn···C	336[c]	60 ± 20	6.0 ± 0.2
AN[d]	0.229	Mn−N	222 ± 1	67 ± 3	6[e]
PN[d]	0.217	Mn−N	221 ± 1	66 ± 3	6.0[f]
BuN[d]	0.205	Mn−N	221 ± 1	69 ± 3	6.1[f]
^{i}BuN[d]	0.208	Mn−N	221 ± 1	67 ± 3	5.9[f]
VN[d]	0.200	Mn−N	220 ± 1	64 ± 3	6.1[f]
BzN[d]	0.100	Mn−N	221 ± 1	50 ± 6	5.7[f]

[a] Determined by the X-ray diffraction technique. [b] In mol dm^{-3}. [c] Restricted as r(Mn−N) + 115 pm. [d] Determined by the EXAFS technique with $E_0 = 6555.6 \pm 0.2$ eV and $\lambda = 622 \pm 10$ pm. [e] Fixed during a least-squares calculation. [f] With several % errors.

For the NMR measurements, the dilution of the above solution and the transfer into an NMR sample tube were performed under a dry nitrogen atmosphere. The sample solutions for variable-temperature NMR measurements were degassed and sealed in an 8-mm o.d. NMR tube. The tube was inserted into a 10-mm o.d. NMR tube, and a deuterated solvent (a mixture of D_2O and ethylene glycol for the measurement above 80 °C; D_2O for between 20 and 80 °C; acetone-d_6 for below 20 °C) containing a trace amount of CH_3NO_2 as a reference of the chemical shift was placed in the outer tube. The sample solutions for variable-pressure NMR measurements were filled in a 7-mm o.d. glass NMR tube with a flexible Teflon cap.[7,16] The concentrations of the sample solutions for the NMR measurements are given in Table S1 (see Supporting Information).

The AN solution of the manganese(II) ion (0.465 mol dm^{-3}) for the XD measurements and the six nitrile solutions for the EXAFS measurements were prepared by the same method as the samples for the NMR measurements. The concentrations of the manganese(II) ion are given in Table 1.

X-ray Diffraction Measurements and Data Analysis. XD measurements were performed at 23 °C on a $\theta-\theta$ type diffractometer (RINT 1100S, Rigaku, Tokyo) equipped with a Mo tube ($\lambda = 0.7107$ Å). Scattered X-ray radiation was monochromatized by a Johansson type graphite monochromator and detected by a scintillation counter. The accessible range of the scattering angle (2θ) was from 2 to 140°, which corresponds to the scattering vector ($s = 4\pi\lambda^{-1} \sin\theta$) range of $(0.3-16.6) \times 10^{-2}$ pm^{-1}. The times required to collect 120 000 counts were recorded at each 2θ angle, and the measurement was repeated three times.

The scattered intensities were corrected for background, absorption, polarization, and double scattering of X-rays and then scaled to the absolute intensities $I(s)$ by comparing the experimental values with the calculated coherent intensities in a region of large scattering angles ($\theta > 50°$).[17] The obtained scaling factor was within 2% agreement with that calculated by the integration method.[18] The structure function, $i_{obsd}(s)$, was obtained by subtracting the independent scatterings as

$$i_{obsd}(s) = I(s) - \sum_j N_j\{(f_j(s) + \Delta f_j')^2 + (\Delta f_j'')^2 + \Phi(s) I_j^{inco}(s)\} \quad (1)$$

where N_j is the number of j atoms in a stoichiometric volume, V, containing one manganese(II) ion, $f_j(s)$ is the atomic scattering factor, and $\Delta f_j'$ and $\Delta f_j''$ are the real and imaginary parts of the anomalous dispersion, respectively. $\Phi(s)$ is the fraction of the total incoherent scattering reaching the detector and $I_j^{inco}(s)$ is the incoherent scattering

(9) (a) Swift, T. J.; Connick, R. E. *J. Chem. Phys.* **1962**, *37*, 307. (b) McConnell, H. M. *J. Chem. Phys.* **1958**, *28*, 430.
(10) Ohtaki, H.; Radnai, T. *Chem. Rev.* **1993**, *93*, 1157.
(11) Ozutsumi, K.; Koide, M.; Suzuki, H.; Ishiguro, S. *J. Phys. Chem.* **1993**, *97*, 500.
(12) Aizawa, S.; Matsuda, K.; Tajima, T.; Maeda, M.; Sugata, T.; Funahashi, S. *Inorg. Chem.* **1995**, *34*, 2042.
(13) Kurihara, M.; Ozutsumi, K.; Kawashima, T. *J. Sol. Chem.* **1995**, *24*, 719.
(14) Inada, Y.; Sugimoto, K.; Ozutsumi, K.; Funahashi, S. *Inorg. Chem.* **1994**, *33*, 1933.
(15) Funahashi, S. *High-Pressure Liquids and Solutions*; Taniguchi, Y., Senoo, M., Hara, K., Eds.; Elsevier: New York, 1994.
(16) Ishii, M.; Funahashi, S.; Ishihara, K.; Tanaka, M. *Bull. Chem. Soc. Jpn.* **1989**, *62*, 1852.
(17) (a) Milberg, M. E. *J. Appl. Phys.* **1958**, *29*, 64. (b) Azaroff, L. U. *Acta Crystallogr.* **1955**, *8*, 701. (c) Warren, B. E.; Mozzi, R. L. *Acta Crystallogr.* **1966**, *21*, 459.
(18) (a) K.-Moe, *J. Acta Crystallogr.* **1956**, *9*, 951. (b) Norman, N. *Acta Crystallogr.* **1957**, *10*, 370.

intensity. The values of $f_j(s)$ and $I_j^{inco}(s)$ for the neutral atoms and those of $\Delta f_j'$ and $\Delta f_j''$ were the values reported in the literature.[19]

The theoretical structure function, $i_{calc}(s)$, resulting from the interatomic interaction is calculated as

$$i_{calc}(s) = \sum_{j,k,j\neq k} \frac{n_{jk}}{r_{jk}s}[\{f_j(s) + \Delta f_j'\}\{f_k(s) + \Delta f_j'\} + (\Delta f_j'')(\Delta f_j'')]\sin(r_{jk})\exp(-b_{jk}s^2) \quad (2)$$

where r_{jk}, b_{jk}, and n_{jk} are the distance, the temperature factor, and the number of atom pairs $j-k$, respectively. A least-squares refinement of the structure parameters, r_{jk}, b_{jk}, and n_{jk}, was carried out to minimize the error-squares sum of $\sum s^2\{i_{obsd}(s) - i_{calc}(s)\}^2$ after trial-and-error estimations of the structure model so as to produce a smooth background curve of the radial distribution function obtained by the Fourier transformation. Calculations were performed using the program KURVLR.[20]

EXAFS Measurements and Data Analysis. The sample solutions for EXAFS measurements were absorbed in porous glass disks (radius = 2 cm and thickness = 2 mm) which were sealed with PET film in order to prevent moisture ingress and evaporation of the solvent. X-ray absorption spectra were measured in the vicinity of the manganese K edge using the BL-6B station at the Photon Factory of the National Laboratory for High Energy Physics.[21] The incident X-ray intensity, I_0, and the transmitted intensity, I, were simultaneously measured by the ionization chambers in lengths of 17 and 31 cm, filled with N_2 gas and with a 1:3 mixture of Ar and N_2 gas, respectively.

The details of the EXAFS data analysis were the same as previously reported.[14,22] The normalized EXAFS oscillation function, $\chi_{obsd}(k)$, was Fourier transformed, and the structure parameters were determined using the Fourier-filtered $k^3\chi(k)$ values. The model function of the EXAFS oscillation, $\chi_{calc}(k)$, is given as[23]

$$\chi_{calc}(k) = \sum_j \left\{\frac{n_j}{kr_j^2}\right\} \exp\left(-2\sigma_j^2k^2 - \frac{2r_j}{\lambda}\right) F_j(\pi,k)\sin\{2kr_j - \alpha_j(k)\} \quad (3)$$

where $F_j(\pi,k)$ is the back-scattering amplitude from each of n_j scatterers j at distance r_j from the X-ray absorbing atom. σ_j is the Debye−Waller factor, λ is the mean free path of a photoelectron, and $\alpha_j(k)$ is the total phase shift. $F_j(\pi,k)$ and $\alpha_j(k)$ were cited from the literature.[24] The parameters E_0 and λ were determined from the EXAFS spectrum of the AN solution as the standard sample on the basis of the structure parameters determined by the XD method. The obtained values of E_0 and λ were kept constant in the course of the structural analysis of the other nitriles, and the values of r_j, σ_j, and n_j were optimized as variables by a curve fitting procedure. Calculations were performed using the program REX (Rigaku, Tokyo).

Treatments of NMR Data. Nitrogen-14 NMR measurements were carried out using JNM-GX270 and JNM-FX100 FT-NMR spectrometers (JEOL, Tokyo) operating at 19.52 and 7.20 MHz, respectively. For the AN solution, the carbon-13 NMR measurements decoupled with ^{1}H nuclei were also performed at 67.94 MHz. The temperature was measured by a substitution technique with a thermistor sensor. For the high-pressure NMR measurements, the pressure generated by a high-pressure pump was measured with a Heise Bourdon gauge, and poly(chlorotrifluoroethylene) was used as the pressure-transmitting medium.[7,16]

The transverse relaxation rate (T_{2P}^{-1}) and the chemical shift ($\Delta\omega_P$) caused by the paramagnetic manganese(II) ion were obtained as

$$(T_{2P}P_M)^{-1} = \pi(\Delta\nu_{samp} - \Delta\nu_{solv})P_M^{-1} \quad (4)$$

$$\Delta\omega_P P_M^{-1} = 2\pi(\omega_{samp} - \omega_{solv})P_M^{-1} \quad (5)$$

where $\Delta\nu$ and ω are the width at half-height and the frequency of an NMR peak for the observed nuclei in the bulk, respectively; the subscripts "samp" and "solv" represent the sample solution in the presence and the absence of the manganese(II) ion, respectively, and P_M is the mole ratio of the coordinated solvent to the bulk solvent. The values of $(T_{2P}P_M)^{-1}$ and $\Delta\omega_P P_M^{-1}$ were, respectively, expressed as eqs 6 and 7 in terms of the transverse relaxation rate in the first

$$(T_{2P}P_M)^{-1} = \tau_M^{-1}\frac{T_{2M}^{-2} + (T_{2M}\tau_M)^{-1} + \Delta\omega_M^2}{(T_{2M}^{-1} + \tau_M^{-1})^2 + \Delta\omega_M^2} + T_{2O}^{-1} \quad (6)$$

$$\Delta\omega_P P_M^{-1} = \frac{\Delta\omega_M}{(1 + T_{2M}^{-1}\tau_M)^2 + (\tau_M\Delta\omega_M)^2} + \Delta\omega_O \quad (7)$$

coordination sphere (T_{2M}^{-1}) and in the outer sphere (T_{2O}^{-1}), the difference in the chemical shift between the coordinated and bulk nitriles ($\Delta\omega_M$), and the mean residence time of a coordinated nitrile on the manganese(II) ion (τ_M).[9] In the present case of the manganese(II) ion, the term $\Delta\omega_M$ could be neglected in eq 6 as will be discussed later.

The temperature dependence of k_{ex} ($= \tau_M^{-1}$), T_{2O}^{-1}, $\Delta\omega_M$, and $\Delta\omega_O$ is expressed as follows;[25] where k_B is the Boltzman constant, h is the

$$k_{ex} = \frac{k_BT}{h}\exp\left(-\frac{\Delta H^{\ddagger}}{RT} + \frac{\Delta S^{\ddagger}}{R}\right) \quad (8)$$

$$T_{2O}^{-1} = C_O\exp\left\{\frac{E_O}{R}\left(\frac{1}{T} - \frac{1}{298.15}\right)\right\} \quad (9)$$

$$\Delta\omega_M = \omega_I\frac{g_e\mu_B}{\gamma_I}\left(\frac{2\pi A}{h}\right)\frac{S(S+1)}{3k_BT} \quad (10)$$

$$\Delta\omega_O = C_{\omega O}\Delta\omega_M \quad (11)$$

Plank constant, R is the gas constant, ω_I is the resonance frequency, g_e is the g value of an electron, μ_B is the Bohr magneton, γ_I is the magnetogyric ratio, $2\pi A/h$ is the hyperfine coupling constant, C_O, E_O, and $C_{\omega O}$ are constants. The term T_{2M}^{-1} was treated by eq 12 for the manganese(II) ion on the basis of the scalar relaxation mechanism,[9,26−28]

$$T_{2M}^{-1} = \frac{S(S+1)}{3}\left(\frac{2\pi A}{h}\right)^2\frac{1}{T_{1e}^{-1} + \tau_M^{-1}} \quad (12)$$

where S is the electronic quantum number and T_{1e}^{-1} is the electronic longitudinal relaxation rate of the manganese(II) ion. In eq 12, T_{1e}^{-1} was treated as nearly the same as the electronic transverse relaxation rate, T_{2e}^{-1}, and its temperature dependence was determined by Purcell and Marianelli to be $4.5\times10^7\exp(292/T)$ in AN.[26]

(19) (a) *International Tables for X-ray Crystallography*; Kynoch Press: Birmingham, 1974; Vol. 4. (b) Cromer, D. T.; Lieberman, D. *J. Chem. Phys.* **1970**, *53*, 1891.
(20) Johansson, G.; Sandström, M. *Chem. Scr.* **1973**, *4*, 195.
(21) Nomura, M.; Koyama, A.; Sakurai, M. *KEK Report 91-1*; National Laboratory for High Energy Physics: Tsukuba, Japan, 1991.
(22) (a) Inada, Y.; Ozutsumi, K.; Funahashi, S.; Soyama, S.; Kawashima, T.; Tanaka, M. *Inorg. Chem.* **1993**, *32*, 3010. (b) Inada, Y.; Funahashi, S. *Anal. Sci.* **1997**, *13*, 373.
(23) (a) Sayers, D. E.; Stern, E. A.; Lytle, F. W. *Phys. Rev. Lett.* **1971**, *27*, 1204. (b) Stern, E. A. *Phys. Rev. B* **1974**, *10*, 3027. (c) Lytle, F. W.; Sayers, D. E.; Stern, E. A. *Phys. Rev. B* **1975**, *11*, 4825. (d) Stern, E. A.; Sayers, D. E.; Lytle, F. W. *Phys. Rev. B* **1975**, *11*, 4836. (e) Lengeler, B.; Eisenberger, P. *Phys. Rev. B* **1980**, *21*, 4507. (f) Lee, P. A.; Citrin, P. H.; Eisenberger, P.; Kincaid, B. M. *Rev. Mod. Phys.* **1981**, *53*, 769.
(24) McKale, A. G.; Veal, B. W.; Paulikas, A. P.; Chan, S.-K.; Knapp, G. S. *J. Am. Chem. Soc.* **1988**, *110*, 3763.
(25) (a) Bertini, I.; Luchinat, C. *NMR of Paramagnetic Molecules in Biological Systems*; Benjamin: California, 1986. (b) Mason, J. *Multinuclear NMR*; Plenum Press: New York, 1987. (c) Harris, R. K. *Nuclear Magnetic Resonance Spectroscopy*; John Wiley & Sons: New York, 1986.
(26) Purcell, W. L.; Marianelli, R. S. *Inorg. Chem.* **1970**, *9*, 1724.
(27) Goldammer, E. V.; Bassaris, C. *J. Sol. Chem.* **1980**, *9*, 237.
(28) Vigee, G. S.; Watkins, C. L.; Harris, M. E. *J. Inorg. Nucl. Chem.* **1980**, *42*, 1441.

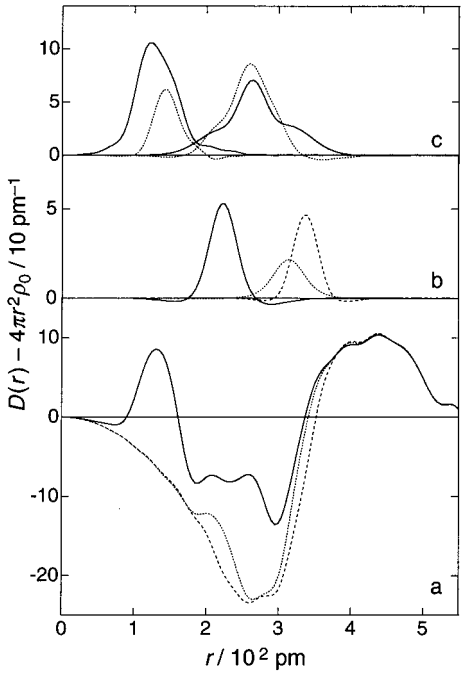

Figure 1. The $D(r) - 4\pi r^2\rho_0$ curve for AN solution of manganese(II) ion. (a) Dashed and dotted lines represent the residual curves after subtraction of the theoretical peaks in b and c, respectively, from the original one (solid line). (b) The theoretical peaks for the Mn−N (solid line), N···N (dotted line), and Mn···C (broken line) interactions around the manganese(II) ion. (c) The peaks for intramolecular interactions within AN molecules (solid lines) and $CF_3SO_3^-$ ions (dotted lines).

The variable-pressure ^{14}N NMR measurements have been performed at around 272 K. The pressure dependence of τ_M^{-1} can be expressed as

$$\tau_M^{-1} = \tau_M(0)^{-1}\left(-\frac{\Delta V^{\ddagger}}{RT}P\right) \qquad (13)$$

where $\tau_M(0)^{-1}$ is the value of τ_M^{-1} at zero pressure and $\Delta V^{\ddagger}$ is the volume of activation. The pressure dependence of T_{2P}^{-1} was then analyzed using eqs 6, 12, and 13. Unfortunately, the variable-pressure NMR measurements for BzN could not be carried out at 272 K because the solution was frozen at elevated pressures. Observed NMR data ($\Delta\nu_{solv}$, $\Delta\nu_{samp}$, ω_{solv}, and ω_{samp}) at various temperatures and pressures are given in Tables S2−S9.

Results and Discussion

Solvation Structures of Mn(II) Ion in Nitriles. Figure 1 shows the radial distribution function in the form of $D(r) - 4\pi r^2\rho_0$ for the AN solution ($V = 3.57 \times 10^9$ pm^3). There are three peaks around 130, 210, and 260 pm. A large broad peak around 400 pm originates from the intermolecular interactions of AN in the bulk. In order to deduce the structure of the solvated manganese(II) ion, the peak shapes due to the intramolecular interactions of the AN molecule and $CF_3SO_3^-$ ion were subtracted from the observed radial distribution function on the basis of reported structures,[29,30] assuming that the temperature factors are 10 pm^2 for the C−F, S−O, and S−C bonds, 30 pm^2 for the F···F, O···O, C···O, and S···F interactions, and 60 pm^2 for the F···O interaction.

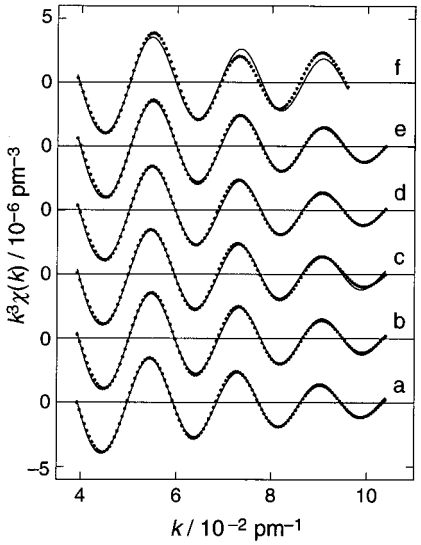

Figure 2. The Fourier-filtered $k^3\chi(k)$ values (dots) and the solid lines for $k^3\chi_{calc}(k)$ depicted using the structure parameters in Table 1. AN (a), PN (b), BuN (c), ^{i}BuN (d), VN (e), and BzN (f).

Subtraction of the calculated peak shapes due to the intramolecular interactions of AN molecules and $CF_3SO_3^-$ ions from the original curve (the solid line in Figure 1a) gave the residual curve (the dashed line in Figure 1a), where the peak remaining at 220 pm was ascribed to the Mn−N interactions in solvated manganese(II) ions. The peak was best reproduced in terms of the presence of six Mn−N bonds with the length of 220 pm. Further subtraction of the peaks due to the N···N and Mn···C(cyano) nonbonding interactions based on the octahedral geometry around the manganese(II) ion led to a smooth background curve (the dotted line in Figure 1a) without a distinct peak over the range of $r < 400$ pm. To refine the structure parameters of the solvated manganese(II) ion, a least-squares calculation was applied to the high-angle region of $si(s)$ values ($s > 4 \times 10^2$ pm^{-1}). In the course of the refinement, the structure parameters of the AN molecule and $CF_3SO_3^-$ ion were fixed by the literature values, and the parameters for the Mn−N, Mn···C(cyano), and N···N interactions were optimized. The structure parameters obtained are given in Table 1.

The observed EXAFS oscillations weighted by k^3, the Fourier transforms, and the Fourier-filtered ($80 < r$/pm < 210) and the calculated EXAFS oscillations are depicted in Figure S1, Figure S2, and Figure 2, respectively. The structure parameters around the manganese(II) ion determined by the least-squares calculations are summarized in Table 1. The fact that the r value of 222 ± 1 pm in AN is in excellent agreement with that determined by the XD method supports the valid estimation of E_0 and λ. In the case of the BzN solution, the relatively low quality of the EXAFS data comes from the low solubility of the manganese(II) salt in BzN. The solvation number, n, is 6 and the Mn−N bond length, r, is 221 ± 1 pm in all nitriles. It is then concluded that the manganese(II) ion in all the present nitriles is solvated by six nitrile molecules with octahedral geometry. The molar volumes of the nitriles are gradually increased as follows: 52.9 for AN, 70.9 for PN, 87.9 for BuN, 90.3 for ^{i}BuN, 104.6 for VN, and 103.1 cm^3 mol^{-1} for BzN. This increase arises from the size of the cyano group substituent. Because the coordinated nitriles are radially expanded from the manganese(II) center, the difference in size of a substituent does not affect the solvation geometry of the manganese(II) ion in the ground state in these nitriles.

(29) (a) Kratochwill, A.; Weidner, J. U.; Zimmermann, H. *Ber. Bunsenes. Phys. Chem.* **1973**, *77*, 408. (b) Radnai, T.; Itoh, S.; Ohtaki, H. *Bull. Chem. Soc. Jpn.* **1988**, *61*, 3845.

(30) (a) Spencer, J. B.; Lundgren, J.-O. *Acta Crystallogr., Sect. B* **1973**, *29*, 1923. (b) Deacon, G. B.; Raston, C. L.; Tunaley, D.; White, A. H. *Aust. J. Chem.* **1979**, *32*, 2195. (c) Åkesson, R.; Sandström, M.; Stålhandske, C.; Persson, I. *Acta Chem. Scand.* **1991**, *44*, 165.

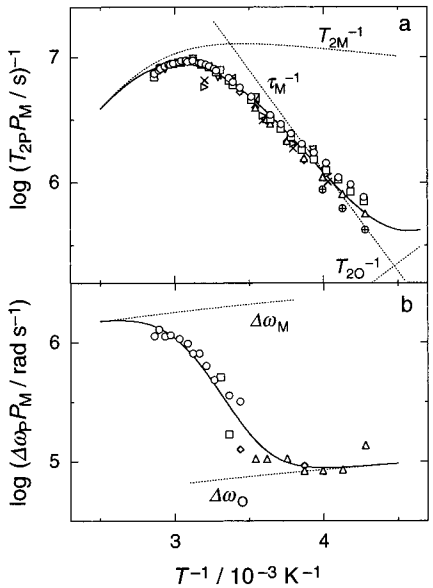

Figure 3. Values of $\log(T_{2P}P_M/s)^{-1}$ (a) and $\log(\Delta\omega_M P_M/\text{rad s}^{-1})$ (b) as a function of the reciprocal of temperature for AN solution of the manganese(II) ion. In Figure 3a, the values for the ^{14}N NMR measurements at 19.52 MHz (○, $P_M = 9.46 \times 10^{-5}$; □, $P_M = 2.76 \times 10^{-4}$; △, $P_M = 4.98 \times 10^{-4}$; ◇, $P_M = 7.31 \times 10^{-4}$; ⊕, $P_M = 2.47 \times 10^{-3}$) and 7.20 MHz (▽, $P_M = 9.46 \times 10^{-5}$; left-pointing triangle, $P_M = 2.76 \times 10^{-4}$) and the ^{13}C NMR measurements at 67.94 MHz (right-pointing triangle, $P_M = 9.46 \times 10^{-5}$; ×, $P_M = 2.76 \times 10^{-4}$) are included. The solid lines represent the calculated curves using the parameters in Table 2.

The solvation structures of the 6-coordinate manganese(II) ion in several nonaqueous solvents with a nitrogen donor atom have been previously reported.[12,13] In aliphatic amines such as trimethylenediamine and propylamine, the Mn−N bond lengths are 228 and 227 pm, respectively,[12] whereas the bond lengths are 225 and 224 pm in 4- and 3-methylpyridines, respectively.[13] Interestingly, the Mn−N bond length becomes longer in the order of nitriles with sp nitrogen < pyridine derivatives with sp^2 nitrogen < aliphatic amines with sp^3 nitrogen. The increase in p character for the lone-pair orbital of the solvent molecules causes expansion of the electron density distribution and places the manganese(II) ion far away from the nitrogen atom. In addition to the nature of the σ donating orbital, the order of π accepting ability is also consistent with the order of the Mn−N bond length. Because the π accepting character on the nitrogen atom is in the order of nitriles > pyridine derivatives > aliphatic amines, the Mn−N bond length in the nitriles is the shortest among these solvents.

Temperature and Pressure Dependence of T_{2P}^{-1} and $\Delta\omega_P$. Figure 3 shows the temperature dependences of T_{2P}^{-1} and $\Delta\omega_P$ in AN. In Figure 3a, the values of $\log(T_{2P}P_M/s)^{-1}$ for ^{14}N NMR measurements at two magnetic frequencies and for ^{13}C NMR measurements are summarized. Because the $\log(T_{2P}P_M/s)^{-1}$ values for the ^{14}N NMR measurements are in excellent agreement with each other, it has been confirmed that $\Delta\omega_M$ can be neglected in eq 6. As apparent from Figure 3, the chemical exchange region is observed at lower than 290 K where the $\Delta\omega_P$ values become nearly flat. Furthermore, the T_{2P}^{-1} values for the ^{13}C NMR at lower than 290 K are in agreement with those for the ^{14}N NMR. These findings support the belief that the relaxation mechanism postulated in this study is valid in AN. The activation parameters of the AN exchange on the manganese(II) ion are almost consistent with those in previous studies (see Table 2).[31] Temperature dependences of $\log(T_{2P}P_M/s)^{-1}$ in PN, BuN, ^{i}BuN, VN, and BzN are shown in Figure S3.

Table 2. Rate Constants at 298 K and Activation Parameters for Nitrile Exchange on Manganese(II) Ion[a]

solvent	k_{ex}^{298} (s^{-1})	$\Delta H^{\ddagger}$ (kJ mol^{-1})	$\Delta S^{\ddagger}$ (J mol^{-1} K^{-1})	$\Delta V^{\ddagger}$ (cm^3 mol^{-1})
AN[b]	1.3×10^7	28.6 ± 0.5	-13 ± 2	-5.8 ± 0.2 [c]
AN[d]	1.4×10^7	29.6	−9	−7.0
AN[e]	1.2×10^7	30.3	−8	
AN[f]	3.1×10^7	35.9	19	
PN	1.3×10^7	29.6 ± 0.7	-10 ± 3	-2.1 ± 0.4 [g]
BuN[h]	9.9×10^6	31.3 ± 0.8	-6 ± 3	-5.0 ± 0.8 [i]
^{i}BuN	1.1×10^7	40.0 ± 0.4	24 ± 1	-2.5 ± 0.7 [j]
VN	9.3×10^6	35.6 ± 0.7	8 ± 3	$+0.6 \pm 0.6$ [k]
BzN	1.2×10^7	36.9 ± 0.8	14 ± 3	

[a] Values of $2\pi A/h$ were 24.1 ± 0.4, 21.4 ± 0.4, 21.8 ± 0.3, 21.6 ± 0.2, 21.0 ± 0.3, and 21.1 ± 0.2 MHz for AN, PN, BuN, ^{i}BuN, VN, and BzN, respectively. [b] The value of $C_{\omega O}$ was $(3.6 \pm 0.2) \times 10^{-2}$. The T_{2O}^{-1} term was fixed using that determined in BuN. [c] At 271.2 K. [d] Reference 5. [e] Reference 26. [f] Reference 28. [g] At 272.0 K. [h] C_O and E_O were $(1.5 \pm 0.2) \times 10^4$ s^{-1} and 15 ± 3 kJ mol^{-1}, respectively. [i] At 272.2 K. [j] At 271.9 K. [k] At 271.4 K.

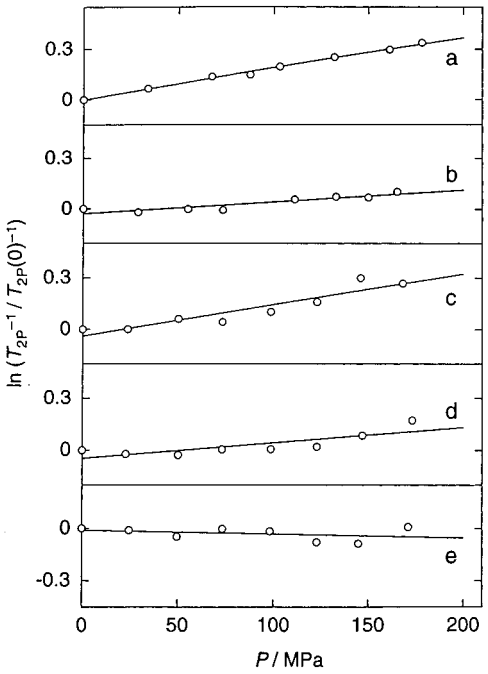

Figure 4. Values of $\ln(T_{2P}^{-1}/T_{2P}(0)^{-1})$ as a function of pressure for AN (a), PN (b), BuN (c), ^{i}BuN (d), and VN (e) solutions of the manganese(II) ion. The solid lines are the curves calculated using the parameters in Table 2.

These data have been analyzed using eqs 6, 8, 9, and 12. For the analysis for PN, BuN, ^{i}BuN, VN, and BzN, we have assumed that the temperature dependence of T_{1e}^{-1} is the same as that in AN. For the manganese(II) ion, T_{1e}^{-1} is interpreted by a modulation of the quadratic zero field splitting,[26] which is related to the structure around the manganese(II) center. As shown above, the solvation structures, especially the Mn−N bond lengths, are almost the same in all nitriles. Thus, the temperature dependence of T_{1e}^{-1} is reasonably accepted to be the same for all nitriles used in this study.

In Figure 4 are plotted the values of $\ln(T_{2P}P_M/s)^{-1}$ as a function of pressure. In the previous study about the AN

(31) Activation parameters of AN exchange in ref 28 obtained from 60 MHz ^{1}H NMR data seem to be less accurate than those in ref 5 and the present study estimated from ^{14}N NMR data. As we have measured ^{14}N and ^{13}C NMR over the wider range of the manganese(II) ion concentration (4×10^{-4} to 10^{-2} mol kg^{-1}), the activation parameters of AN exchange obtained in this work are thought to have higher accuracy.

exchange at the manganese(II) ion, Sisley *et al.* directly determined $\Delta V^{\ddagger}$ from the pressure dependence of $\ln(T_{2P}P_M/s)^{-1}$ assuming the pressure independence of T_{1e}.[5] Under our experimental conditions, the contribution of τ_M^{-1} to the $\ln(T_{2P}P_M/s)^{-1}$ value has been estimated to be *ca.* 75, 72, 79, 83, and 82% for AN, PN, BuN, ^{i}BuN, and VN, respectively. Thus, the contribution of the pressure dependence of T_{1e}^{-1} to the $\Delta V^{\ddagger}$ values should be as small as in the case of Sisley *et al.* The small pressure dependence of T_{1e}^{-1} was also suggested for the water exchange of the polyaminopolycarboxylatolanthanide(III) complexes.[32] The obtained activation parameters for the nitrile exchange are summarized in Table 2.

Reaction Mechanisms of Nitrile Exchange. The recent theoretical calculations have pointed out that the bond lengths of the remaining solvent molecules, which do not participate in the exchange reaction, are not changed for the associative activation process.[3a,b,i] It is important to define "the inner sphere" of the solvated metal ion, that is, the effective sphere into which solvent molecules in the bulk cannot penetrate at the ground state.[16,33] Under such circumstances, $\Delta V^{\ddagger}$ can be regarded as the difference between the positive contribution to the volume due to the dissociation of a leaving solvent from the inner sphere and the negative contribution due to an entering ligand into the inner sphere. In a series of solvents with different bulkiness, we must consider the difference in the size of the inner sphere due to the bulkiness of the solvent molecules. Thus, we first discussed the mechanisms for the nitrile exchange in terms of the $\Delta H^{\ddagger}$ values.

The donor number, which is a good measure of the differences in the Mn−N bond energies,[34] is 14.1 for AN, 16.1 for PN, 16.6 for BuN, 15.4 for ^{i}BuN, and 11.9 for BzN.[35] The small difference in the donor number suggests that the Mn−N bond energies are regarded as being nearly the same, because the solvation structures in all nitriles are the same on the basis of the EXAFS results. Thus, we can accept the assumption that the Mn−N bond energies in the ground state are identical for all nitriles.

In the case of the smallest AN, we have come to the conclusion that the AN exchange on the manganese(II) ion proceeds *via* the associative interchange pathway on the basis of the negative values of $\Delta V^{\ddagger}$ and $\Delta S^{\ddagger}$ and the small value of $\Delta H^{\ddagger}$, similar to the conclusion of a previous study.[5] As shown in Table 2, the value of $\Delta H^{\ddagger}$ gradually increases in the order of AN < PN < BuN < VN < BzN < ^{i}BuN. Because of the similar Mn−N bond energies for all nitriles, the increase suggests that the reaction mechanism of the nitrile exchange becomes less associative from AN to ^{i}BuN. This order is consistent with that of the bulkiness of the nitrile molecules. The mechanism of the nitrile exchange then becomes less associative due to the steric hindrance in the transition state. The molecules with a bulky substituent such as BzN and ^{i}BuN seem to have the greatest disadvantage for the associative mode of activation. Referring to the theoretically calculated structure of the transition state in the course of the associative interchange mechanism,[3a,b] the steric repulsion between an entering and a leaving solvent molecule is thought to be serious for these nitriles with a branch. The less dissociative character in BzN rather than in ^{i}BuN is interpreted as being due to a planar substituent, the phenyl group, of BzN, in contrast to the bulkier isobutyl substituent of ^{i}BuN. The value of $\Delta S^{\ddagger}$ is increased in response to the increase in $\Delta H^{\ddagger}$ and then the values of $\Delta G^{\ddagger}$ are very near constant for the reactions investigated. Such an isokinetic relationship with the isokinetic temperature 306 K (Figure S4) indicates the change in mechanism from associative to less associative in response to the increase in bulkiness of the nitrile molecules.

The change in reaction mechanism with the bulkiness of the nitrile molecules also appears in the variation of the $\Delta V^{\ddagger}$ values. The $\Delta V^{\ddagger}$ value in PN is less negative than that in AN and that in VN is more positive than that in BuN. The $\Delta V^{\ddagger}$ value in PN, however, is less negative than that in BuN, though the reaction mechanism of the PN exchange is thought to be more associative than the BuN exchange on the basis of the values of $\Delta H^{\ddagger}$ and $\Delta S^{\ddagger}$. The decrease in $\Delta V^{\ddagger}$ from PN to BuN can be attributed to the increase in the radius of the inner sphere around the manganese(II) ion, *i.e.*, the size of the inner sphere is thought to be in the order of AN ∼ PN < BuN ∼ VN < ^{i}BuN. An expansion of the inner sphere can make $\Delta V^{\ddagger}$ more negative in the case of the associative activation process. The volume decrease due to an entering BuN may be larger than the corresponding decrease for PN, whereas the entering BuN molecule is farther from the manganese(II) ion than in the case of PN. On the other hand, the volume increase due to a leaving nitrile should not be significantly influenced by the expansion of the inner sphere because of the cylindrical form of the nitrile molecule. Thus, if the difference in the volume decrease due to an entering nitrile overcomes the difference in the volume increase due to a leaving nitrile, there is the possibility of a more negative $\Delta V^{\ddagger}$ value for a less associative mechanism.

Acknowledgment. This work was supported by Grants-in-Aid for Scientific Research (Nos. 07454199, 07504003, and 09874131) from the Ministry of Education, Science, Sports, and Culture of Japan. The EXAFS measurements were performed under the approval of the Photon Factory Program Advisory Committee (Proposal No. 92G179).

Supporting Information Available: The concentrations of the sample solutions for the NMR measurements (Table S1), observed NMR data ($\Delta\nu_{solv}$, $\Delta\nu_{samp}$, ω_{solv}, and ω_{samp}) at various temperatures and pressures (Tables S2−S9), observed EXAFS oscillations (Figure S1), Fourier transform magnitudes (Figure S2), values of $\log(T_{2P}P_M/s)^{-1}$ plotted against the reciprocal of temperature (Figure S3), and isokinetic relationship (Figure S4) (11 pages). Ordering information is given on any current masthead page.

IC970830M

(32) (a) Micskei, K.; Helm, L.; Brücher, E.; Merbach, A. E. *Inorg. Chem.* **1993**, *32*, 3844. (b) Pubanz, D.; González, G.; Powell, D. H.; Merbach, A. E. *Inorg. Chem.* **1995**, *34*, 4447. (c) Powell, D. H.; Ni Dhubhghaill, O. M.; Pubanz, D.; Helm, L.; Lebedev, Y. S.; Schlaepfer, W.; Merbach, A. E. *J. Am. Chem. Soc.* **1996**, *118*, 9333. (d) Tóth, É.; Burai, L.; Brücher, E.; Merbach, A. E. *J. Chem. Soc., Dalton Trans.* **1997**, 1587.
(33) Jordan, R. B. *Inorg. Chem.* **1996**, *35*, 3725.
(34) Gutmann, V. *The Donor−Acceptor Approach to Molecular Interactions*; Plenum Press: New York, 1978.
(35) Riddick, J. A.; Bunger, W. B.; Sakano, T. K. *Organic Solvents: Physical Properties and Methods of Purification*, 4th ed.; John Wiley & Sons: New York, 1986.